

Calculation of Scalars in Neugebauer-Like Models. II: Final Scalar Function is Copula

J. A. Stephen Viggiano[^]

School of Photographic Arts and Sciences, Rochester Institute of Technology
E-mail: jasvppr@rit.edu

Abstract. *Neugebauer-type models for reflectance factor spectra produced by halftone-based color hardcopy rely on the spectra of the so-called Neugebauer primaries, an invertible function of reflectance, and a weight, or scalar, for each Neugebauer primary. This paper discusses the calculation of the third factor. Research has, until now, relied heavily, perhaps exclusively, on just three parameter-less sets of equations to compute these scalars. In the previous paper in this series, it was shown how the scalar for each Neugebauer primary could be computed from the function governing the scalar of the primary consisting of all colorants, the so-called final scalar. In this paper, conditions necessary and sufficient for a function to provide the final scalar are recited. Copulas, an entire class of functions from probability theory, also satisfy these conditions, and therefore may be used for final scalar calculation. Halftone patterns generated by a raster image processor were used to assess potential improvement in final scalar accuracy in two-colorant dot-on-dot printing with a slight amount of misregistration. Using a copula new to this application resulted in a nearly ten-fold improvement in accuracy over the best-performing overlap models in the prior art, indicating significant increases in accuracy are to be expected with actual printed artifacts. © 2018 Society for Imaging Science and Technology.*
[DOI: 10.2352/J.ImagingSci.Technol.2018.62.5.050403]

1. INTRODUCTION

1.1 From Part I

In the previous paper in this series [1], a model for reflectance spectra of halftone-based color hardcopy, referred to as a *Neugebauer-type model*, was introduced. It generalizes similar models by admitting alternative mappings of reflectance, in addition to the power law first suggested for wide-band reflectometry by Yule et al. [2, 3], and, though not new, factored out specific formula for the scalars (weights, or area fractions) for each Neugebauer primary.

The point of the previous paper was to disclose that all scalars or weights in Neugebauer-type models may be written in terms of a single function that defined the overlap behavior. Instances of this function were identified for conventionally angled screens, dot-on-dot screening, and, for the two-colorant case, dot-off-dot screening. The motivation for this was to enable easy substitution of new and different models for halftone dot overlap, with potential for increased characterization accuracy of halftone-based color hardcopy.

[^] IS&T Member.

Received Apr. 15, 2018; accepted for publication July 15, 2018; published online Sep. 12, 2018. Associate Editor: Chunhui Kuo.

1062-3701/2018/62(5)/050403/8/\$25.00

Several modifications [4–11] of the classic model for reflectance spectra of color halftones [12, 13] were discussed; speculation was offered that these modifications were necessitated by failure of the “classic three” models of halftone dot overlap (Demichel, Dot-on-dot, and dot-off-dot). Indeed, the work of Bala explicitly mentions (and addresses) this.

A program written in the Python programming language was also described. This program generates code for a function in Python that computes each of the scalars. The arguments to the function are the area fractions of each colorant and a pointer to a specific overlap function. The program is open-source, and available at <https://sourceforge.net/projects/neugebauerscalar>.

1.2 Objectives

The major goal for this paper is to enumerate the properties of functions necessary and sufficient for them to be used for scalar calculation in Neugebauer-type models. These properties are shared with a class of functions already known in probability theory, and so this class of functions will be identified.

Secondary goals include an experimental proof of concept to illustrate the value of the new capability, and suggestions for possible ways to apply the method.

1.3 How this Paper is Organized

In the next section, some properties common to existing final scalar functions are enumerated, and it is shown that they are not sufficient to guarantee a function may be used to compute valid scalars. In the section that follows, an additional property, subtler and at the same time more complicated, is identified. A set of conditions sufficient for a function to produce valid scalar values is recited at the end of that section.

In the section “Final Scalar is a Copula,” the class of functions that satisfy these conditions are identified. The instances in the prior art are identified, and examples from probability literature but new to this context are introduced.

An experiment, based on actual halftone bitmaps, was conducted to serve as proof of concept and illustrate potential accuracy increase.

Two strategies for more complex situations are discussed in the section that follows the experiment. A pair of screening scenarios are presented, and a promising copula-*cum*-final scalar function is identified for each.

In the final section, future work, including the following paper in the series, is discussed.

SYMBOLS AND NOTATION

(Some of the notation that follows differs from that conventionally used in copula literature. This is to avoid collision with nomenclature customarily used in print modeling literature. Thus, the customary C for copula is replaced with F ; M for the Fréchet upper bound is replaced with A (points up), etc.)

i : Number of colorants (inks); number of random variables in a random vector

p : Number of Neugebauer primaries (usually 2^i)

c, m, \dots, k : A list of i colorant amounts

a_j : Scalar multiplier for the j th Neugebauer primary; conceptually, the area fraction covered by that primary

$[x, y]$: Interval from x to y ; all real numbers equal to or greater than x and less than or equal to y . When $x < y$ the interval is *nondegenerate*.

I : Unit interval $[0, 1]$; all real numbers between zero and one

F : Function for the p^{th} (final) scalar, also a *copula*, an i -variate cumulative distribution function (CDF) whose marginal distributions are all uniform on I

Π : Copula for independent random variables; final scalar for conventionally angled screens

A : Upper-bound copula; final scalar for dot-on-dot screening

V : Copula lower bound; final scalar for 2-colorant dot-off-dot screening

The convention $F(x, y, \dots; \theta, \varphi)$ will be used to distinguish variables in the list of arguments to a function F from parameters. Variables will be enumerated before the semicolon, while parameters (normally held constant) will come after the semicolon.

2. PROPERTIES OF THE FINAL SCALAR FUNCTION F

The final scalar function, $F(c, m, \dots, k)$ is an i -place function of the colorant amounts, each of which is between zero and one, that results in the weight or scalar for (conceptually, the area fraction occupied by) the Neugebauer primary consisting of all i colorants. The result must also lie between zero and one. Symbolically, $F: I^i \rightarrow I$. In the previous paper, it was shown that the Final scalar function may be used to compute *all* scalars, not just the final scalar.

Key properties of this function are identified and described in the remainder of this section and in the following section.

2.1 Overarching Property

Not every i -place function that maps the unit square, cube, or hypercube to the unit interval $[0, 1]$ may be used. An overarching property, one that dominates all others, is that

the function F cannot assume a value that results in a negative scalar for any Neugebauer primary. While this precludes any function that is negative for any combination of ink amounts in I^i , this restriction has further reach. It was shown in the previous paper in this series that *all* scalars may be written in terms of the function F , so this function may not return a value that results in a negative scalar resulting even indirectly.

The final scalar for Demichel's solution (for any number of colorants), for dot-on-dot (again, for any number of colorants), and for true dot-off-dot (which only exists for $i = 2$) all obey the following three key properties:

2.2 Nondecreasing in Each Ink Amount

While one need not necessarily see an increase in the final scalar when the level of one colorant is increased (but the others remain constant), there should certainly be no decrease. The function F must be nondecreasing in each colorant amount.

2.3 Margins

If all but one of the colorant amounts are 1, the area fraction of the final primary will be the amount of the colorant that is not maxed out. Clearly, if all but one colorant have complete coverage of a region, the area of the overlap of them and the remaining colorant will be the area of the remaining colorant.

Similarly, if all of the colorant amounts are unity, the final scalar will itself be 1.

2.4 Minimum Colorant Amount as Upper Bound

The relative area covered by all colorants at once can be no greater than the relative area covered by any of them. Symbolically:

$$F(c, m, \dots, k) \leq \min(c, m, \dots, k).$$

A consequence of this is that the final scalar for dot-on-dot is the upper bound for all final scalars.

A special case of this property is presented next as another feature of this function and to more easily rule out candidate functions that do not satisfy it. This additional property is:

2.4.1 Grounding.

F will equal zero if one or more of its arguments are zero, because of this upper bound. Logically, if at least one of the colorant amounts is zero, all colorants cannot appear.

2.5 Insufficiency of These Properties

The three key properties enumerated above (nondecreasing in each colorant amount, margins, and minimum colorant amount as upper bound) do not guarantee that the overarching property is satisfied.

Consider the following function for two colorants, C and M ; the amounts of each are c and m , respectively:

$$F_t(c, m) = \max \left[0, \frac{9(c + m - 1) - 5cm}{3 + c + m - cm} \right]. \quad (1)$$

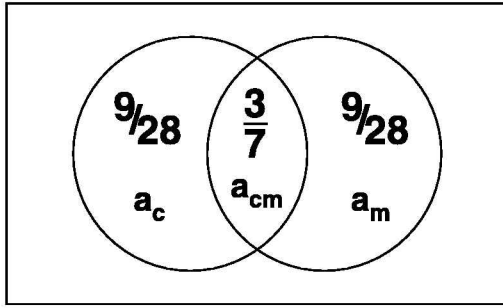


Figure 1. Nonpaper scalars using illegal final scalar function. The scalars for the C, M, and CM primaries are shown for $c = m = 3/4$, using Eq. (1). While the three scalars shown are all between 0 and 1, they sum to more than 1, leaving a negative amount $(-1/14)$ for the paper.

It can be shown that F_t is nondecreasing in each colorant amount, obeys the margin property, and never exceeds $\min(c, m)$. Evaluating the function at $c = m = 3/4$ yields $3/7$. This is a_{cm} , the scalar for the two-colorant CM primary. The colorant amount c is the sum of a_{cm} and a_c , the scalar for the C primary. This latter scalar is obtained by subtraction, yielding $a_c = 9/28$. The scalar for the M primary has the same value. (Refer to Figure 1.) All of these scalars are between zero and one, and, so far, all appears well. However, the three values sum to $15/14$, resulting in a scalar for the remaining primary (the paper) of $-1/14$.

Because the function F_t results in the calculation of a negative scalar amount, it cannot be a valid choice for a final scalar function. In the following section, an additional property is identified, which generalizes the nondecreasing property and therefore replaces it.

3. *i*-NONDECREASING PROPERTY

In the previous section, it was shown that the three enumerated properties do not guarantee that a function is useable to calculate scalars. In this section, an additional property of the final scalar function is identified. This property subsumes the nondecreasing in each colorant amount property, and so will replace it. Because it may be new to many readers, is somewhat involved, and is pivotal in this paper, it is addressed separately.

3.1 Difference Operator

Define the operator $\Delta_{u_1}^{u_2}$ as

$$\Delta_{u_1}^{u_2} G(u) = G(u_2) - G(u_1),$$

where G is a function of u and other variables whose values remain fixed. Clearly, if G is nondecreasing in u , then, for $u_2 > u_1$, $\Delta_{u_1}^{u_2} G(u) \geq 0$. In the next sections, this nondecreasing property in one variable is extended to 2-nondecreasing (nondecreasing in two variables) and *i*-nondecreasing (nondecreasing in *i* variables).

3.2 2-Nondecreasing Property

Let G be a function of two variables, c and m . Let c_1 and c_2 be particular values of c , with $c_2 > c_1$, and m_1 and

m_2 be particular values of m with $m_2 > m_1$. Say that G is 2-nondecreasing in c and m if and only if the forward difference

$$\begin{aligned} \Delta_{c_1}^{c_2} \Delta_{m_1}^{m_2} G(c, m) &= \Delta_{c_1}^{c_2} [G(c, m_2) - G(c, m_1)] \\ &= [G(c_2, m_2) - G(c_2, m_1)] \\ &\quad - [G(c_1, m_2) - G(c_1, m_1)] \\ &= G(c_2, m_2) - G(c_2, m_1) \\ &\quad - G(c_2, m_1) + G(c_1, m_1) \end{aligned} \quad (2)$$

is not negative for all possible values of $c_1 < c_2$ and $m_1 < m_2$.

3.3 Transition to Higher Dimensionality

To ease the transition to higher dimensionality, note that the function G is evaluated at the vertices of the rectangle defined by the Cartesian product of the two nondegenerate intervals $[c_1, c_2]$ and $[m_1, m_2]$.

Note that the terms in the final expression in Eq. (2) are assigned a negative sign if the number of left endpoints (c_1, m_1) are odd, and positive if the number of left endpoints are even.

3.4 *i*-Nondecreasing Property

Let G be a function of *i* variables, c, m, \dots, k . Let $[c_1, c_2]$ be a nondegenerate interval in the variable c , $[m_1, m_2]$ be a nondegenerate interval in the variable m , and so on. If the condition

$$\Delta_{c_1}^{c_2} \Delta_{m_1}^{m_2} \dots \Delta_{k_1}^{k_2} G(c, m, \dots, k) \geq 0 \quad (3)$$

is satisfied for all possible nondegenerate intervals in c, m, \dots, k , then the function G is termed *i*-nondecreasing.

Just as it was possible to write the second-order mixed difference in Eq. (2) as the sum of the function evaluated at the vertices of a rectangle, weighted by either +1 or -1, so to it is possible to write the condition as

$$\sum_{\mathbf{v} \in \mathbf{V}} s(\mathbf{v}) G(\mathbf{v}) \geq 0, \quad (3a)$$

where \mathbf{V} is the set of all vertices of the *i*-dimensional hyperbox formed by the Cartesian product $[c_1, c_2] \times [m_1, m_2] \times \dots \times [k_1, k_2]$, and $s(\mathbf{v})$ is +1 if the number of left endpoints in vertex $\mathbf{v} \in \mathbf{V}$ is even and -1 if odd.

Example 1. The two-place function F_t given in Eq. (1) is not 2-nondecreasing, because

$$\begin{aligned} \Delta_{3/4}^1 \Delta_{3/4}^1 F_t(c, m) &= F_t(1, 1) - F_t\left(1, \frac{3}{4}\right) \\ &\quad - F_t\left(\frac{3}{4}, 1\right) + F_t\left(\frac{3}{4}, \frac{3}{4}\right) \\ &= 1 - \frac{3}{4} - \frac{3}{4} + \frac{3}{7} \\ &= \frac{-1}{14} < 0. \end{aligned}$$

Example 2. Consider the function

$$F_g(c, m) = \max \left[0, \frac{4(c + m - 1) + 5cm}{8 + c + m - cm} \right]. \quad (4)$$

It can be proven (the proof is tedious if it is not to depend on concepts beyond the scope of this paper; a very simple proof hinges on this function being an *Archimedean copula* with generator $\psi(u) = (1 - u)/(2 + u)$) that the function in Eq. (4) satisfies the upper bound, margins, and 2-nonincreasing properties.

3.5 F is i -Nondecreasing

One additional property is that F be i -nondecreasing. While it is necessary that the area fraction of this final primary may not decline as any single colorant amount is increased, it is also necessary that the scalar for (area fraction of) the all-colorant primary may not decrease as any combination of colorant amounts is increased. If the i -nondecreasing property is satisfied, that is, if

$$\Delta_{c_1}^{c_2} \Delta_{m_1}^{m_2} \dots \Delta_{k_1}^{k_2} F(c, m, \dots, k) \geq 0$$

for all $0 \leq c_1 < c_2 \leq 1, 0 \leq m_1 < m_2 \leq 1, \dots, 0 \leq k_1 < k_2 \leq 1$, no scalar may decrease as any combination of colorant amounts are increased.

It has been proven [14, Lemma 2.10.3, p. 44] that this property ensures the function is nondecreasing in any combination of its arguments. This stronger nondecreasing property therefore subsumes the requirement for F to be nondecreasing in each individual colorant amount, and thus replaces it.

3.6 Final Enumeration of Properties

A function $F : I^i \rightarrow I$ that:

1. satisfies the marginal property; i.e., if all but one colorant amount is unity, the function evaluates as the remaining colorant amount;
2. satisfies the upper-bound property; i.e., $F(c, m, \dots, k) \leq \min(c, m, \dots, k)$
3. is i -nondecreasing

will generate valid scalar values.

These conditions constitute the necessary and sufficient conditions for a function to generate valid scalar values. Additional properties include grounding (if any colorant amount is zero, $F = 0$), nondecreasing in each variable, and uniform continuity on its domain, I^i [14, p. 46].

4. FINAL SCALAR FUNCTION IS A COPULA

Functions that satisfy the properties listed immediately above are called *copulas*, and have been studied extensively. In essence, a copula is an i -variate CDF whose marginal distributions are all continuous uniform distributions on the unit interval. An introduction to copulas is provided by Nelsen [14].

The name “copula,” from the Latin word for link or tie, was first used by mathematician Abraham Sklar [15], who later related that he borrowed the word from linguistics.

4.1 Copulas Already used as Final Scalar Functions

There are three copulas already used for scalar calculation. The prior art consists of:

4.1.1 Demichel Equations; Pi or Independence Copula

M. E. Demichel provided an early model of dot overlap [16, 17] that was used by Neugebauer [18] in his eponymous model. The final scalar function is simply the product of the colorant amounts. This is referred to as the “Pi copula” [14, p. 12, p. 47] or *Independence copula* in copula literature:

$$a_{cm\dots k} = \Pi(c, m, \dots, k) = c \cdot m \cdot \dots \cdot k. \quad (5)$$

As shown in the previous paper in this series, the remaining scalars may be computed from this function, yielding the familiar Demichel equations:

$$\begin{aligned} a_w &= (1 - c)(1 - m) \dots (1 - k) \\ a_c &= c(1 - m) \dots (1 - k) \\ &\vdots \end{aligned}$$

This copula is applicable to conventionally angled clustered-dot screens, and uncorrelated FM screening. Nevertheless, this author suspects it is applied when many other types of screening are used for lack of a better alternative.

4.1.2 Dot-on-dot; Upper-Bound Copula

Bala [5] disclosed a model for dot-on-dot screening, wherein the screens share the same screen frequency, screen orientation, and phase (i.e., they have common centers). The scalar for the i th primary may be written as:

$$a_{cm\dots k} = A(c, m, \dots, k) = \min(c, m, \dots, k). \quad (6)$$

This is known as the *Fréchet upper bound* in copula literature, after a theorem in an article [19] written by him.

4.1.3 Dot-off-dot; Lower Bound

If two screen patterns have the same frequency and angle, but have the center of the dark dot for one colorant co-located with the center of the light hole for the other, the final scalar may be calculated:

$$a_{cm} = V(c, m) = \max(0, c + m - 1). \quad (7)$$

While this expression is a specialization of the more general

$$V(c, m, \dots, k) = \max(0, c + m + \dots + k - i + 1), \quad (8)$$

where, as before, i is the number of colorants, V is a copula, and will generate valid scalars, when $i = 2$, but not when $i > 2$. It nevertheless is the lower bound for copulas; for some c, m, \dots, k , there will exist a copula F' such that $F'(c, m, \dots, k) = V(c, m, \dots, k)$ [14, pp. 47–48]. Accordingly, this function is referred to as the *Fréchet lower bound* in copula literature.

While this author is unable to locate a reference for use of this in the prior art, it had nevertheless been employed in

unpublished software at RIT Research Corporation. It would seem likely this model had been employed by others, as well.

4.2 Examples of Other Copulas useful in Scalar Calculation

4.2.1 Archimedean Copula with First-order Rational Generator

The copula given in Eq. (4) is a specialization of

$$F_r(c, m; \theta) = \max\left(0, \frac{\theta^2(c+m+1) + (2\theta+1)cm}{\theta(\theta+2) + c+m-cm}\right) \quad (9)$$

with $\theta = 2$. Valid values for the parameter are non-negative. (The counter-example F_t given in Eq. (1) used a negative value, -3 for the parameter, breaking the copula.)

This copula is valid only for two colorants (except as $\theta \rightarrow 0$), but may have utility in situations like rational tangent screening.

4.2.2 Gaussian Copula

Let \mathbf{P} be an $i \times i$ correlation matrix, Φ^{-1} be the inverse univariate standard Gaussian CDF, and $\Phi(c, m, \dots, k; \mathbf{0}, \mathbf{P})$ be the i -variate Gaussian CDF with mean of zero for all variates and covariance matrix \mathbf{P} . Then

$$F_G(c, m, \dots, k; \mathbf{P}) = \Phi\left(\Phi^{-1}(c), \Phi^{-1}(m), \dots, \Phi^{-1}(k); \mathbf{0}, \mathbf{P}\right). \quad (10)$$

This copula is versatile, with $i(i-1)/2$ parameters; the only restriction is that the correlation matrix be symmetric with no negative eigenvalues. It is therefore expected to be adaptable to a wide variety of screening conditions.

4.2.3 Frank Copula

Frank [20] suggested an associative copula, containing a single parameter:

$$F_F(c, m, \dots, k; \theta) = -\frac{1}{\theta} \ln\left(1 + \frac{(e^{-\theta c} - 1)(e^{-\theta m} - 1) \dots (e^{-\theta k} - 1)}{(e^{-\theta} - 1)^{i-1}}\right) \quad (11)$$

where $\theta \neq 0$ is a parameter. As $\theta \rightarrow 0$, $F_F \rightarrow \Pi$, the independence copula that generates the Demichel equations; as $\theta \rightarrow \infty$, $F_F \rightarrow A$, the upper-bound copula that generates the scalars for dot-on-dot; and as $\theta \rightarrow -\infty$, $F_F \rightarrow V$, the lower bound. Therefore, the Frank copula generalizes all three.

5. EXPERIMENTAL

The question to be addressed is, “Can a copula provide greater accuracy than the traditional models for halftone dot overlap (Demichel, dot-on-dot, and dot-off-dot)?” A computational experiment was conducted as a proof of concept for copulas in calculating scalars in Neugebauer-like models. Because all $p = 2^i$ scalars may be computed using the

function for the final scalar, the accuracy of all scalars hinges on the accuracy of this final scalar.

5.1 Approach

While evaluating different copulas using scalars computed from actual printed samples might have greater relevance, these are early days for copulas in this application, and something closer to a proof of concept, with actual known ground truth, was deployed here.

The approach was:

- Generate halftone bitmaps.
- Combine them in pairs to generate a bitmap for a two-colorant overlap.
- Count pixels in the source bitmaps and in the overlap bitmap to know, with certainty, the colorant amounts and the area fraction for the two-colorant primary.
- Estimate, using traditional overlap models (Demichel, dot-on-dot, and dot-off-dot), the area fraction of the two-colorant Neugebauer primary.
- Estimate, using a copula, the same area fraction.
- Compare the estimates with the ground truth values.

A simulation was performed using halftone patterns generated by a raster image processor. This modality was selected to avoid uncertainty injected by photometric measurements, variation of inking levels, nonuniformity in the substrate, and other sources. One set of nine bitmaps (nominal area fractions from 10 to 90%, in 10% increments) were generated for the first colorant, and a second set was generated for the second colorant. The fraction of “on” pixels was counted in each bitmap, yielding the actual amounts of each colorant. A pair of bitmaps, one bitmap from each set, were logically “ANDed” together to produce a bitmap representing the two-colorant primary. The fraction of “on” pixels was counted in this two-colorant primary bitmap, yielding the scalar for the final primary. Each bitmap from the first set was combined in this manner with each bitmap in the second set, yielding 81 pairs.

5.2 Specific Methodology

A page description file was written in the Postscript language. The halftone screen was specified using the `setscreen` operator, using a screen angle of 0° , a frequency of 0.01 times the bitmap addressability, resulting in a 100×100 pixel halftone cell (a complete halftone cell occupied a slightly larger area, possibly because of rounding error), and the so-called “Diamond” spot function [21, p. 66], a best-in-class spot function that produces diamond-shaped dots in the midtones and circular dots in the highlights and shadows. Nine halftone patterns, with nominal colorant amounts between 10 and 90 % in 10 % increments, were generated. Each pattern spanned more than six halftone cells in both width and height.

Samples, each two halftone cells in both height and width (201 pixels square), were cropped from each pattern. Two different origins were used to simulate a slightly

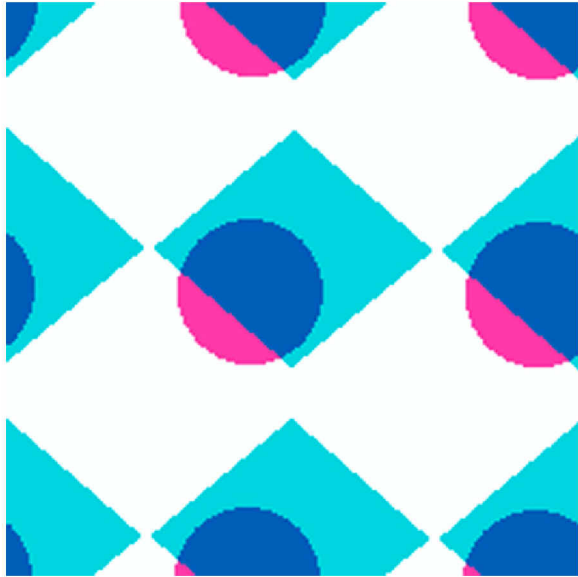


Figure 2. Sample bitmap combination. Example bitmaps from experiment, showing misregistration of Cyan and Magenta dot-on-dot screening. Colorant amounts, based on pixel counting, are $c = 0.3966$, $m = 0.1973$; area fraction of overlap $a_{cm} = 0.1481$.

misregistered dot-on-dot screening arrangement. (With no misregistration, the upper-bound copula, A , would predict the overlap fractions within rounding error; the remaining copulas would produce varying degrees of error for this ideal but difficult to meet in practice scenario.) The patterns for the first colorant (cyan) were offset by 0.15 times the halftone pitch in the vertical direction, while the patterns for the second colorant (magenta) were offset by this same distance, but horizontally. An example pair is shown in Figure 2.

The command-line tool “pamcrop” from the netpbm [22] suite was used to perform the cropping under the supervision of a Debian Almquist shell script. A second script supervised the Boolean “AND” operation to generate the pixelmap of the overlap region (using netpbm program “pamarith”) and compute the fraction of foreground pixels (using netpbm program “pamsumm”) in the individual bitmaps (to provide ground truth for the colorant amounts c and m) as well as in the overlap bitmaps (providing the ground truth for the scalar a_{cm}).

5.3 Copulas Exercised

The three copulas used in the prior art (lower bound/dot-off-dot, upper bound/dot-on-dot, and independence/conventionally angled screens) were exercised, as well as the Frank copula in Eq. (11), using a parameter $\theta = 4$. This value was selected because the overlap was, due to misregistration, between dot-on-dot ($\theta \rightarrow \infty$) and dot-off-dot ($\theta \rightarrow -\infty$), but closer to the latter.

As each “ANDed” image was generated, the colorant amount values and scalar (area fraction of overlap) were written to a text file. The text file was then processed by a

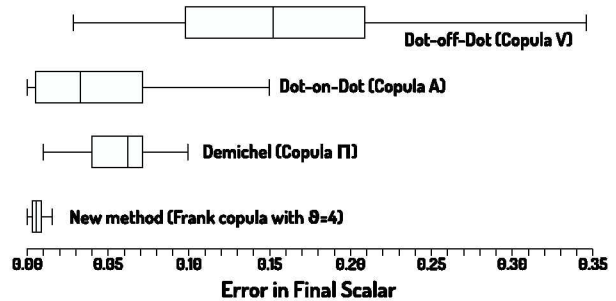


Figure 3. Boxplots of errors. Boxplots of errors in final scalar for four copulas. The top three use overlap models in the prior art; the bottom boxplot shows the error using the new method.

script in the Python programming language that evaluated each copula at each of the 81 combinations of c and m and computed the difference from the ground truth measured from the overlap bitmap.

5.4 Results

The results are summarized as boxplots (each showing minimum, first quartile, median, third quartile, and maximum errors) in Figure 3, and as error maps in Figure 4. As expected, the lower-bound copula V , which models dot-off-dot, performed quite poorly, with a root mean square error (RMSE) of 0.1763. The upper-bound copula A , appropriate for dot-on-dot, performed better, with an RMSE of 0.0605. The classic Demichel equation, as the independence or Π copula, had a similar RMSE of 0.0617.

In sharp contrast, the Frank copula with $\theta = 4$, representing the new approach, performed considerably better, with an RMSE of only 0.0074, nearly an order of magnitude better than the best method in the prior art. The maximum error produced using the new approach, 0.0160, was lower than the first quartile error for two of the three prior art models (dot-off-dot and Demichel), and lower than the median error produced by all three models in the prior art.

5.5 Discussion

The scenario of misregistered dot-on-dot screens is more plausible than that of perfect registration. The amount of misregistration is a small fraction (roughly one-fifth) of the halftone pitch, amounting to just 0.036 mm at 150 lines per inch. While it is likely the improvement will be smaller for actual printed dots, the dramatic reduction in error produced using a copula other than one of the “classic three” for a simulation of a very plausible scenario serves as compelling evidence of potential merit for the new approach.

6. COPULAS FOR SPECIFIC OVERLAP SITUATIONS

6.1 CMY dot-on-dot; K off-dot

Conventionally angled screens produce noticeable (and objectionable) rosette patterns on devices with low spatial addressability; desktop printers have employed dot-on-dot

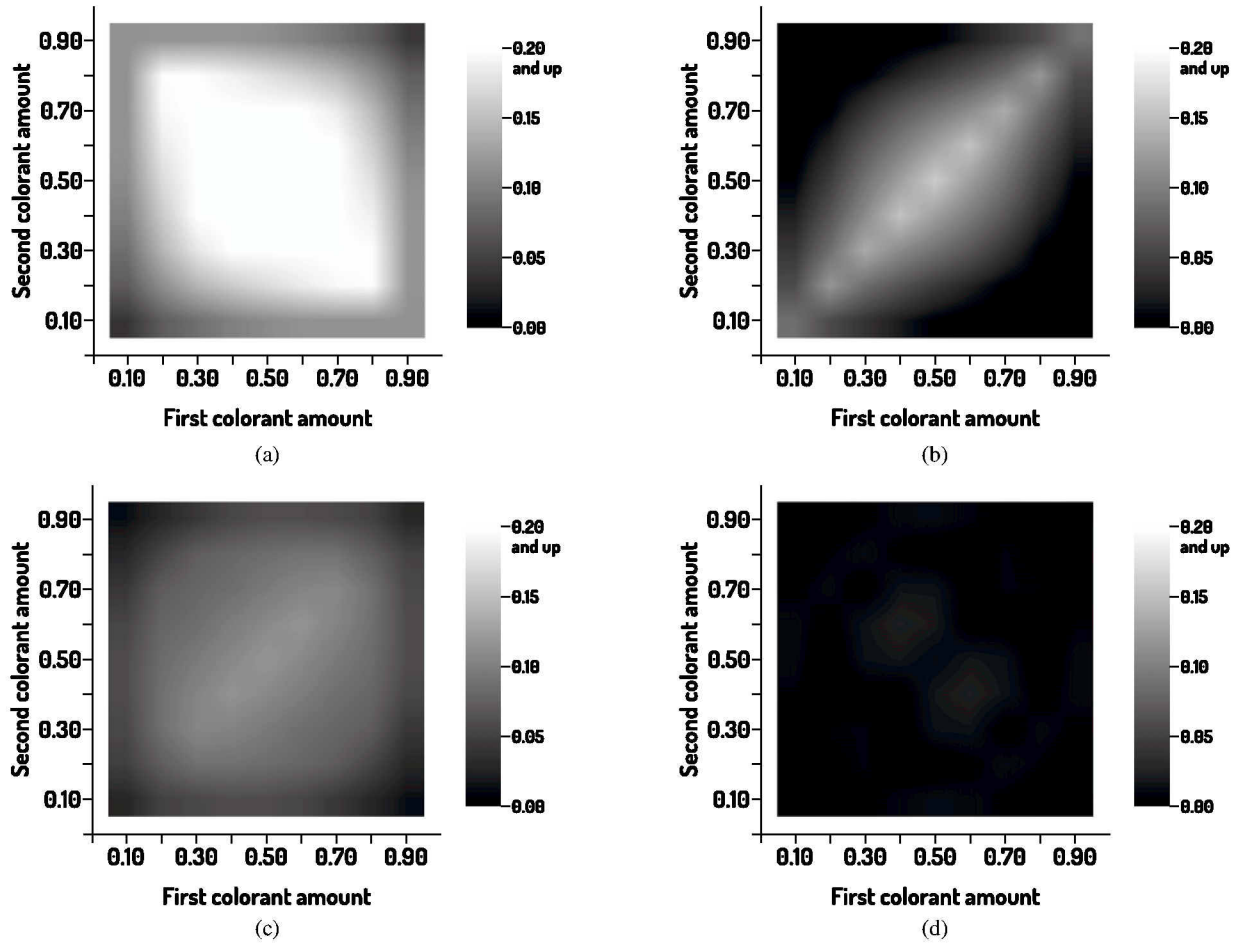


Figure 4. Error maps. Error maps for four copulas against ground truth. (a) Dot-off-dot copula (V). (b) Dot-on-dot copula (A). (c) Independence copula/Demichel equations (Π). (d) Frank copula with $\theta = 4$. Darker is better: Black represents no difference between ground truth and copula-computed scalar; white represents an absolute difference of 0.20 (or greater).

for cyan, magenta, and yellow to eliminate the rosette pattern. If black were to also be printed dot-on-dot, it would tend to cover the other colorants, reducing the gamut. Accordingly, black could be oriented dot-off-dot relative to the other colorants.

A copula to consider in this scenario may be constructed from both bounding copulas, thus:

$$F(c, m, y, k) = V[A(c, m, y), k]. \quad (12)$$

6.2 A Seven-colorant Solution

To minimize moiré in traditional process color separation, the axes of the cyan, magenta, and black are oriented 30 degrees from each other. Because the dots have near bi-axial symmetry, and the human visual system has low acuity in the portion of the spectrum it modulates, the yellow screen is usually oriented with its axes running horizontally and vertically, placing it midway between two of the others [23, 24].

A red separation may be added with minimal impact on moiré by orienting it dot-off-dot relative to one of the other colors. Because they are complementary, it seems logical to pair the red in this manner with cyan. Similarly, the green may be paired dot-off-dot with magenta, and blue with yellow.

A copula for this overlap behavior is

$$F(c, m, y, r, g, b, k) = \Pi[V(c, r), V(m, g), V(y, b), k]. \quad (13)$$

7. CONCLUSIONS AND FUTURE WORK

7.1 Conclusions

Researchers in color models for halftone printing have restricted themselves to consideration of just a few (specifically, three) models for overlap among the dots of different colors. This may be limiting the accuracy of models based on physics.

Conditions necessary and sufficient for a function to compute the final scalar in Neugebauer-type models have

been identified. While the “classic 3” functions extent in the prior art satisfy these conditions, *copulas*, an entire class of functions from probability theory, also satisfy these conditions and may also be used for scalar computation. This opens a new door for improvements to models for reflectance factor spectra produced by halftone-based color hardcopy.

A realistic scenario was simulated to evaluate potential for using copulas beyond the “classic 3.” Employing an alternative copula (Frank’s copula, with parameter $\theta = 4$) resulted in a reduction in RMSE in area fraction of nearly an order of magnitude. While the data were based on halftone bitmaps not printed but directly from a raster image processor, the dramatic improvement in accuracy signals great promise for the new approach.

7.2 Future work: Coming in Part III

The next paper in this series will discuss techniques for selecting copulas for specific situations, and a method for determining values of parameters, because most copulas contain one or more parameters. Additional copulas will be introduced and evaluated. Actual printed halftone patterns, using the diamond spot function employed in the computational experiment in this paper, as well as possibly others, will be analyzed.

Dot shape, controlled by the spot function, may exert a second- (or higher) order effect on overlap. The level of this effect will be assessed by performing computational experiments similar to the one described in this paper, using a variety of common spot functions.

To provide a benchmark, the computational experiment described in this paper will be replicated with no misregistration.

Companion software for parameter determination will be released under an open-source license.

7.3 Additional Future Work

The other feature of Neugebauer-type models, the use of bijective mappings of spectral reflectance factor other than the power law suggested by Yule and Nielsen in 1951, will also be investigated. Piecewise linear, polynomial, and rational functions seem worth considering.

ACKNOWLEDGMENTS

Publication of this paper was enabled by a grant from the Office of the Vice President for Research at the Rochester Institute of Technology; RIT’s College of Art and Design assisted with travel funds to present the paper. The author warmly thanks his colleagues in the School of Photographic Arts & Sciences at RIT and RIT’s Interdisciplinary Copula Reading and Problem Group for their assistance and encouragement.

The author thanks the reviewers of this paper for their thoughtful and timely review, as well as for constructive suggestions that have improved clarity.

Dedication

This paper is dedicated to the memory of advisor, mentor, colleague, and friend, Irving Pobboravsky.

REFERENCES

- ¹ J. A. Stephen Viggiano, “Calculation of scalars in Neugebauer-type models. I: Refactoring the calculations,” *Proc. IS&T CIC25: Twenty-Fifth Color and Imaging Conference* (IS&T, Springfield, 2017), pp. 123–129.
- ² J. A. C. Yule and W. J. Neilsen [sic], “The penetration of light into paper and its effect on halftone reproduction,” *TAGA Proc.* (Technical Association of the Graphic Arts, Rochester, NY, 1951), pp. 65–76.
- ³ J. A. C. Yule and R. Colt, “Colorimetric investigations in multicolor printing,” *TAGA Proc.* (Technical Association of the Graphic Arts, Rochester, NY, 1951), pp. 77–82.
- ⁴ K. J. Heuberger, Z. M. Jing, and S. Persiev, “Color transformations and lookup tables,” *TAGA/ISCC Proc.* (Technical Association of the Graphic Arts, Rochester, NY, 1992), pp. 863–881.
- ⁵ R. Balasubramanian, “Printer model for dot-on-dot halftone screens,” *Proc. SPIE* **2413**, 356–364 (1995).
- ⁶ R. Balasubramanian, “Optimization of the spectral Neugebauer model for printer characterization,” *J. Electron. Imaging* **8**, 156–166 (1999).
- ⁷ R. D. Hersch and F. Cr  t  , “Improving the Yule-Nielsen modified spectral Neugebauer model by dot surface coverages depending on the ink superposition conditions,” *SPIE Color Imaging X* (International Society for Optical Engineering, Bellingham, WA, 2005), Vol. 5667, pp. 434–445.
- ⁸ M. H  bert and R. D. Hersch, “Reflectance and transmittance model for recto-verso halftone prints: spectral predictions with multi-ink halftones,” *J. Opt. Soc. Am. A* **26**, 356–364 (2009).
- ⁹ M. H  bert and R. D. Hersch, “Yule-Nielsen based recto-verso color halftone transmittance prediction model,” *Appl. Opt.* **50**, 519–525 (2011).
- ¹⁰ P. Pjanic and R. D. Hersch, “Specular color imaging on a metallic substrate,” *Proc. IS&T CIC21: Twenty-First Color and Imaging Conf.* (IS&T, Springfield, VA, 2013), pp. 61–68.
- ¹¹ V. Babaei and R. D. Hersch, “Color reproduction of metallic-ink images,” *J. Imaging Sci. Technol.* **60** (2016) 30503.
- ¹² J. A. Stephen Viggiano, “The color of halftone tints,” *TAGA Proc.* (Technical Association of the Graphic Arts, Rochester, NY, 1985), pp. 647–661.
- ¹³ J. A. Stephen Viggiano, “*Models for the Prediction of Color in Graphic Reproduction Technology*”. MSc thesis (Rochester, NY: Rochester Institute of Technology, 1987).
- ¹⁴ R. B. Nelsen, *An Introduction to Copulas*, 2nd ed. (Springer, New York, 2006).
- ¹⁵ A. Sklar, “Fonctions de r  partition    n dimensions et leurs marges,” *Publications de l’Institut de Statistique de l’Universit   de Paris* (Institut de Statistiques de l’Universit   de Paris, Paris, 1959), Vol. 8, pp. 229–231.
- ¹⁶ M. E. Demichel, *Proc  d  * **26**, 17–21 (1924).
- ¹⁷ M. E. Demichel, *Proc  d  * **26**, 26–27 (1924).
- ¹⁸ H. E. J. Neugebauer, “Die theoretischen Grundlagen des Mehrfarbenbuchdrucks,” *Z. W. Photographie Photophysik und Photochemie* **36**, 73–89 (1937).
- ¹⁹ M. Fr  chet, “G  n  ralisations du th  or  me des probabilit  s totales,” *Fundam. Math.* **25**, 379–387 (1935).
- ²⁰ M. J. Frank, “On the simultaneous associativity of $f(x, y)$ and $x + y - f(x, y)$,” *Aequationes Mathematicae* **19**, 194–226 (1979).
- ²¹ P. Fink, *PostScript Screening: Adobe Accurate Screens* (Adobe Press, Mountain View, CA, 1992).
- ²² netpbm (software suite). netpbm.sourceforge.net.
- ²³ J. A. C. Yule, *Principles of Color Reproduction* (Wiley, New York, 1967).
- ²⁴ M. F Southworth, *Color Separation Techniques*, 1st ed. (North American Publishing, Philadelphia, PA, 1974).